Performance of the Barzilai-Borwein fixed-step optimization approach in non-invasive microwave imaging

Tareq F A Zanoon
Computer Systems Engineering Dept.
Arab American University
Jenin, Palestine
tareq.zanoon@aaup.edu

***Abstract*—In this paper, the performance of the Barzilai-Borwein non-line search descent is investigated as an inversion strategy for solving the nonlinear inverse scattering problem of Ultra-Wide Band (UWB) microwave tomographic imaging. The appealing feature of reducing the computational time by avoiding extensive line search calculations is tested. The capability of this method in solving cases of high nonlinearity, due to dense and complicated tissue structures, is evaluated and compared to the classical steepest decent, and the conjugate gradient approaches. Cross-sectional slices of glandular human breast tissue structures derived from MRI numerical data phantoms are used and tested with the presence of cancerous tissue. Reconstructed images are presented and discussed with particular attention to the image reconstruction time, and the accuracy of the outcome. Results indicate that the Barzilai-Borwein fixed-step approach outperforms the others in terms of accuracy, overall convergence, and susceptibility to local minima traps, although requiring a greater number of iterations.**

Keywords—inverse scattering, microwave imaging, image reconstruction, gradient method, Barzilai-Borwein.

I. Introduction

UWB tomography has been investigated as an imaging tool for various medical imaging applications given its safety and low-cost advantages [1-3]. In principle, microwave tomography maps the dielectric characteristics of the media under investigation. Different biological tissues, such as fatty, glandular, normal, and cancerous exhibit different dielectric characteristics based on their structure. Earlier studies confirm this variance over the microwave frequency range [4 -6].

Nevertheless, microwaves do not follow a straight path similar to that of X-Rays, and therefore, the relationship between the scatterer and its response is nonlinear. The challenging aspect of microwave tomographic reconstruction is to solve the inverse scattering problem that is well understood to be ill-posed, and non-linear in nature [7]. For most practical considerations, the presence of stronger scatterers increases the nonlinearity of the problem, thus violating the appealing simplistic linearization assumptions that are known for their low computational cost. Furthermore, attempting to detect smaller targets requires the use of smaller wavelengths, thus increasing the illumination frequency which, in turn, contributes positively towards increasing the nonlinearity of the problem [8]. This is also observed when the imaging domain has multiple scatterers. As the imaging domain becomes more complex, the shortcomings of the linearised solutions and assumptions are more evident.

To resolve such issues, the inverse scattering problem is formed as an optimization problem aiming to obtain a solution that represents the best match between data sets obtained from both measurements and calculations. The inversion can be achieved by minimizing the least squares function defined as the difference between both datasets, where an iterative procedure updates the calculated data in the direction of the minima. Hence, the computational cost involved will depend on the number of iterations, and the computational cost per iteration. This can vary depending on the inversion strategy considered. Gradient methods rely on searching in a direction of the solution at each of its iterations while Newton methods, despite being more superior, have complications associated with computing the Hessian and performing matrix inversion. Other methods, such as the conjugate gradient method, have performance characteristics that are intermediate between the steepest descent and Newton methods. Appealingly, gradients can be easily obtained using the adjoint method as the computational cost is equivalent to that of a single forward-reverse problem runs, regardless of the number of variables.

Nevertheless, a line search method is still required at each iteration. Regardless of the method used, this step is computationally extensive as each point of the line search requires the calculation of the forward problem. To reduce this complexity, it is reasonable to avoid the line search procedure at all if possible, trading it with a fixed-step approach. One of the most appealing methods is the Barzilai-Borwein (BB) fixed-step approach [9-11]. In this paper, we investigate the performance of the BB two-point step size gradient approach in solving the nonlinear inverse scattering problem for microwave tomographic imaging applications, particularly, breast tumor detection in realistic tissue structures.

II. Mathematical Formulation

An ultra wide-band microwave imaging system relies on solving two problems: The direct (forward problem) in which scattered waves are calculated with the spatial dielectric distribution fully known, and the inverse problem which reconstructs the spatial dielectric distribution of the imaging domain utilizing what is known from the scattered wave response. The Mathematical formulation follows the approach in [8] and is presented here for the sake of completeness. A two-dimensional imaging domain Ω is considered with full

978-1-6654-8800-6/22/$31.00 ©2022 IEEE

view scanning geometry. The imaging domain, bounded within the scanners, is completely described in terms of its spatial dielectric distribution $\boldsymbol{x}=(\varepsilon)$.

To solve the inverse problem, an error cost function F is defined as the least squares between the calculated (E^{calc}) and measured (E^{meas}) data sets for each transmitter-receiver pair composing the full view geometry. The objective of the optimization process is to minimize F and solve the unknown spatial dielectric distribution $\boldsymbol{x}=(\varepsilon)$. Assuming a total of M transmitters and N receivers, the residual error of the N receiving locations for the m^{th} projection over the time T in TM mode can be expressed as :

$$r(\boldsymbol{x}) = \frac{1}{2}\sum_{n=1}^{N}\int_T\int_\Omega \left(E_z^{calc}{}_n(\boldsymbol{x}) - E_z^{meas}{}_n\right)^2 d\Omega dt\delta \quad (1)$$

where δ is the Dirac delta function. The cost function for the total M projections can be written as:

$$F(\boldsymbol{x}) = \sum_{m=1}^{M} r_m(\boldsymbol{x}) \qquad (2)$$

where m=1,2,..,M, is the transmitter location.

For the spatial dielectric distribution $\boldsymbol{x}$, the negative of the gradient $\boldsymbol{g} = \nabla F(\boldsymbol{x})$ should point to the maximum rate of decrease of F at $\boldsymbol{x}$, which sets the direction towards the minimizer in our case.

Meanwhile, the gradient can be calculated using the adjoint state method [12]. The adjoint problem is solved by backward time propagation of the residual errors, and is evaluated using the FDTD method in the same way used for the direct problem. Mathematically, the gradient of F with respect to the permittivity of the i^{th} & j^{th} unknowns in a two-dimensional xy plane can be expressed as:

$$\boldsymbol{g} = \nabla F(\boldsymbol{x}) = \sum_{m=1}^{M}\left(\sum_{nt=1}^{NT-1}\sum_{i,j\,\epsilon\Omega}^{Ni\ Nj} e_z \frac{dE_z}{dt}\Delta x\Delta y\,\Delta t\right) (3)$$

where t and E_z represent the time step and electric field along the z direction respectively.

The iterative procedure is started by an initial guess $\boldsymbol{x}_0$ that is usually selected to match the homogeneous medium which comprises the majority of the imaging domain under investigation.

As for the search direction, the classical steepest descent converges orthogonally in the maximum decent direction of F *(*direction of $\boldsymbol{g}_k$ *for the* k^{th} iteration*)*. Conjugate directional methods, on the other hand, compute a conjugate direction for every iteration as the algorithm iterates. For k=1,2,3,.. iterations, the conjugate gradient update is expressed as:

$$\boldsymbol{x}_{k+1} = \boldsymbol{x}_k + \alpha_k \boldsymbol{d}_k \quad (4)$$

where αk is the step size, and dk can be taken as:

$$\boldsymbol{d}_k = \begin{cases} -\boldsymbol{g}_k, & k = 0; \\ -\boldsymbol{g}_k + \beta\boldsymbol{d}_{k-1} & k \geq 1; \end{cases} \quad (5)$$

Here, we consider β_k to be taken according to the Polak-Rebiere's formula given as:

$$\beta_k = \frac{\boldsymbol{g}^{(k)T}\left[\boldsymbol{g}^{(k)} - \boldsymbol{g}^{(k-1)}\right]}{\|\boldsymbol{g}^{(k)}\|^2} \qquad (6)$$

On the other hand, the BB two-point gradient method derives the step size from a two-point approximation of the secant equation underlying quasi-Newton methods, here α_k has a fixed size given as:

$$\alpha_k = \frac{\boldsymbol{S}_{k-1}^T\ \boldsymbol{y}_{k-1}}{\boldsymbol{y}_{k-1}^T\boldsymbol{y}_{k-1}} \quad (7)$$

and

$$\alpha_k = \frac{\boldsymbol{S}_{k-1}^T\ \boldsymbol{S}_{k-1}}{\boldsymbol{S}_{k-1}^T\boldsymbol{y}_{k-1}} \quad (8)$$

where $\boldsymbol{S}_{k-1} = \boldsymbol{x}_k - \boldsymbol{x}_{k-1}$, and $\boldsymbol{y}_{k-1} = \boldsymbol{g}_k - \boldsymbol{g}_{k-1}$. The fixed-step α_k given in equation 7 and equation 8 can be used interchangeably as followed elsewhere [11].

III. METHODS AND SETUP

Following a similar approach to [8], the forward problem setup uses a multistatic configuration with 8 an UWB-transceiver arrangment. The transmitters take turns illuminating the imaging domain in sequence. For each transmitter, seven scattered wave measurements are recorded resulting in an overall of 56 transmitter-receiver pair measurements. The transceivers are arranged equidistantly contouring the imaging domain (Fig. 1). The domain is constructed using 110 x110 FDTD cells of 5mm spatial step size in both dimensions, and a time step of Δt = 8.33 pS. The computational domain is bounded by 10 PML cells in all directions.

A numerical breast model derived from 3 dimensional anatomically realistic breast phantom is used to model breast tissue. This model originates from T1- magnetic resonance images (MRI) and has been transformed into electrical properties [13]. Fig. 2 shows an MRI sagittal slice of a human breast with less than 25% scattered fibro-glandular tissue structure together with their corresponding electrical characteristic transformation obtained at 5 GHz. Figure 3 shows the cross-sectional slice selected from the model.

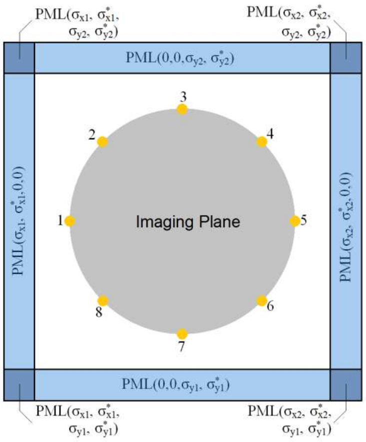

Fig. 1. FDTD computational domain showing the imaging plane, transceiver locations, and perfectly matching layers boundary [8].

Tumors on the other hand are modeled based on studies reported in [14]. Table 1 summarizes these characteristics, while Fig. 4 shows the incorporation of an assumed 1.5 cm tumor in the cross-sectional model. The tumor is located slightly offset to avoid confusion with any possible artifacts.

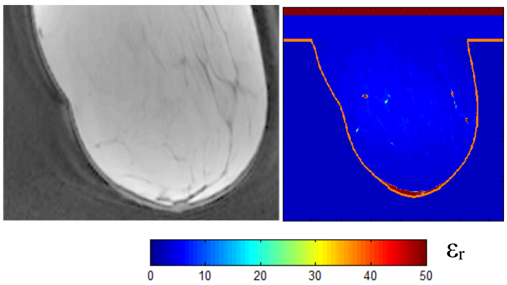

Fig. 2. T1-MRI (left) with less than 25% scattered fibro-glandular tissue structure, and its transformed dielectric properties at 5GHz (right).

TABLE I. DIELECTRIC PROPERTIES OF FEMALE BREAST TISSUE [14]

Tissue type	**Permittivity (relative)**	**Conductivity S/m**
Fat	4-4.5	0.11 - 0.14
Normal Tissue	10-25	0.35 - 1.05
Malignant Tumor	45-60	3.0 - 4.0

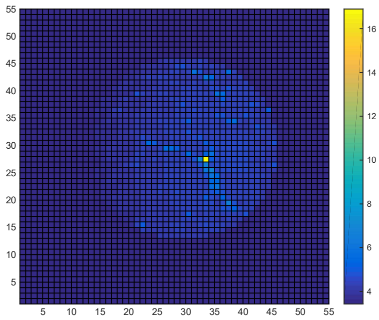

Fig. 3. Cross-sectional slice of healthy breast tissue structure.

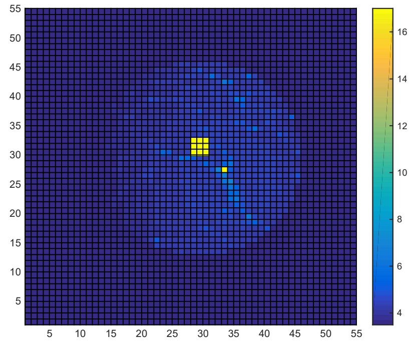

Fig. 4. Incorporating a 1.5 cm malignant tumor in a cross-section healthy breast tissue structure.

IV. RESULTS AND DISCUSSION

The convergence sequence is greatly influenced by the choice of the initial guess used in the first step of the iterative procedure. The most suitable initial guess, in this case, is the homogeneous medium given little is known before the iterative process, which in this case, can only be assumed to be of fatty tissue composition at least. The iterative reconstruction procedure is repeated for the steepest descent, conjugate gradient, and fixed step BB approach attempting to accurately identify and localize the malignant tumor assumed in the numerical model (Fig. 4). A criterion of $< 0.01\%$ of the cost functional error between any two successive iterations was set to terminate the procedures. Figure 5 shows the reconstructed images using each of these approaches.

Examining the results in Fig. 5, a close resemblance can be observed in the reconstructed results in all approaches where the 1.5cm target has been successfully detected and localized. Characteristics of the less distinctive tissue structure are absent, however, concluding that the solutions obtained are not global, but local. This can be further confirmed by examining the convergence trend in Fig. 6 where none of the approaches reach the zero minima.

While the approaches successfully locate the target tumor, the result observed in Fig. 5 (a) appears to be bigger in size and more spread than the actual target. The result obtained by the BB fixed-step and conjugate gradient methods, on the other hand, more accurately depicts the target in the original setup (Fig. 5 (b) and (c)), None of the tested methods manage to capture the internal structure details.

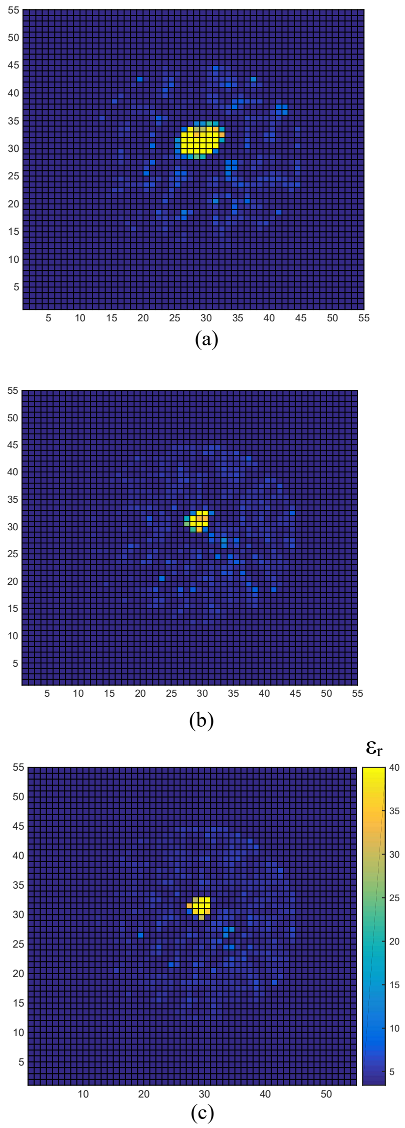

Fig. 5. Reconstructed images featuring (a) Steepest Descent, (b) Conjugate gradient, and (c) Fixed step BB method.

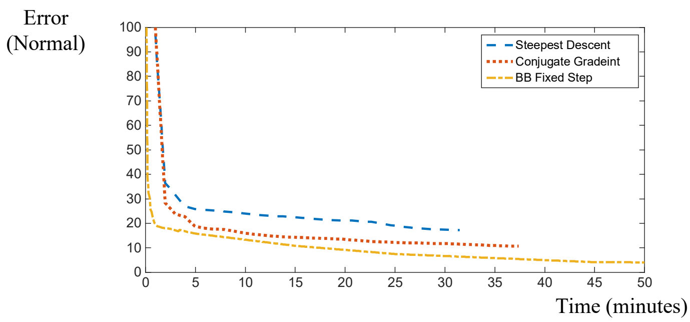

Fig. 6. Convergence trend for Steepest descent, Conjugate gradient, and BB fixed-step approaches.

The accuracy of the BB fixed step method is further confirmed by the convergence trend observed in Fig. 6, where the cost function error resulting from the iterative process is lower in comparison with the other approaches. The approach is also observed to be more immune to local minima traps where iterations continue to reduce the cost function beyond the steepest descent and conjugate gradient approaches.

In terms of computational time, each gradient calculation requires around 6 seconds to compute on an average laptop computer with an i5 CPU and 8 Gbytes RAM. The time required for each fixed-step iteration is around 6 seconds. In contrast, each line search iteration's average time is around 59 seconds. This means that 10 gradients can be computed in the meantime of a single line search iteration.

V. Results and Discussion

The Barzilai-Borwein non-line search descent has been investigated as an inversion strategy for solving the nonlinear inverse scattering problem, and for breast cancer detection in particular. The inversion was applied on anatomically realistic MRI-derived breast phantoms to more accurately resemble the internal structure, embedding an assumed 1.5 cm malignant tumor slightly off the center point. The performance of the mothed was compared to the classical steepest descent and conjugate gradient methods. Results indicate that Barzilai-Borwein fixed-step approach outperforms the others in terms of accuracy and overall convergence, and susceptibility to local minima traps, although requiring a greater number of iterations. Nevertheless, the computational time required for each iteration is significantly less, as the line search procedure is dropped in favor of a fixed step approach, but requires more time in total. However, this might not be the case for higher resolution domains with a significantly higher number of unknowns. This is currently being investigated in our lab.

References

[1] Rafique U, Pisa S, Cicchetti R, Testa O, Cavagnaro M. Ultra-Wideband Antennas for Biomedical Imaging Applications: A Survey. *Sensors,* 22(9):3230, 2022.

[2] Scapaticci, V. Lopresto, R. Pinto, M. Cavagnaro, and L. Crocco, "Monitoring Thermal Ablation via Microwave Tomography: An Ex Vivo Experimental Assessment," Diagnostics, vol. 8, no. 4, p. 81, 2018.

[3] Aldhaeebi MA, Alzoubi K, Almoneef TS, Bamatraf SM, Attia H, M Ramahi O. Review of Microwaves Techniques for Breast Cancer Detection. Sensors. 20(8):2390. 2020.

[4] A. P. O'Rourke, M. Lazebnik, J. M. Bertram, M. C. Converse, S. C. Hagness, J. G. Webster, and D. M. Mahvi, "Dielectric properties of human normal, malignant and cirrhotic liver tissue: in vivo and exvivo measurements from 0.5 to 20 GHz using a precision open-ended coaxial probe," Physics in Medicine and Biology, vol. 52, no. 15, pp. 4707-4719, 2007.

[5] D. Andreuccetti, R. Fossi and C. Petrucci: An Internet resource for the calculation of the dielectric properties of body tissues in the frequency range 10 Hz - 100 GHz. IFAC-CNR, Florence (Italy), 1997. Based on data published by C.Gabriel et al. in 1996.

[6] M. Lazebnik, D. Popovic, L. Mccartney, C. B. Watkins, M. J. Lindstrom, J. Harter, S. Sewall, T. Ogilvie, A. Magliocco, T. M. Breslin, W. Temple, D. Mew, J. H. Booske, M. Okoniewski, and S. C. Hagness, "A large-scale study of the ultrawideband microwave dielectric properties of normal, benign and malignant breast tissues obtained from cancer surgeries," Physics in Medicine and Biology, vol. 52, no. 20, pp. 6093-6115, 2007.

[7] E. Abenius, B. Strand, “Solving inverse electromagnetic problems using FDTD and gradient-based minimization” International Journal for Numerical Methods in Engineering, 68, 650-673, 2006.

[8] Zanoon T., Abdullah M. Early stage breast cancer detection by means of time-domain ultra-wide band sensing. *Meas. Sci. Technol.* 22:114016, 2011.

[9] Raydan, Marcos. The Barzilai and Borwein Gradient Method for the Large Scale Unconstrained Minimization Problem, SIAM Journal on Optimization 7:1:26-33, 1997.

[10] Yakui Huang, Yu-Hong Dai, Xin-Wei Liu, and Hongchao Zhang, On the acceleration of the Barzilai-Borwein method. Comput. Optim. Appl. 81, 3, 717-740, 2022.

[11] Yu-Hong Dai and Roger Fletcher. 2005. Projected Barzilai-Borwein methods for large-scale box-constrained quadratic programming. Numer. Math. 100, 1, 21–47, 2005.

[12] I. T. Rekanos,"Microwave imaging in the time domain of buried multiple scaterrers by using an FDTD-based optimization technique", IEEE Trans. Magn., vol. 29, no. 3, pp. 1381-1384, May 2003.

[13] E. Zastrow, S. Davis, M. Lazebnik, F. Kelcz, B. V. Veen, and S. Hagness, Database of 3 D Grid-Based Numerical Breast Phantoms for use in Computational Electromagnetics Simulations, 2008.

[14] Chaudhary, S. S., Mishra, R. K., Swarup, A. & Thomas, J. M., Dielectric properties of normal & malignant human breast tissues at radiowave & microwave frequencies. *Indian J Biochem Biophys,* 21**,** 76-9, 1984.